The 8th European Congress on Computational Methods in Applied Sciences and Engineering
ECCOMAS Congress 2022
5-–9 June 2022, Oslo, Norway

INTERVAL FIELD METHODS WITH LOCAL GRADIENT CONTROL

Conradus van Mierlo[1], Matthias G.R. Faes[2,1] and David Moens[1]

[1] KU Leuven, Department of Mechanical Engineering, Div. LSMD, Jan de Nayerlaan 5, St-katelijne-waver, Belgium, (koen.vanmierlo, david.moens) [at]kuleuven.be

[2] TU Dortmund University, Chair for Reliability Engineering, Leonhard-Euler-Strasse 5, 44227 Dortmund, Germany, matthias.faes[at]tu-dortmund.de

Key words: Interval fields, Inverse distance weighting, non-deterministic modeling

Abstract.

This paper introduces a novel method to create an interval field based on measurement data. Such interval fields are typically used to describe a spatially distributed non-deterministic quantity, e.g., Young's modulus. The interval field is based on a number of measurement points, i.e., control points, expended throughout the domain by a set of basis functions. At the control point the non-deterministic quantity is known and bounded by an interval. However, at these measurement points information about the gradients might also be available. In addition, the non-deterministic quantity might be described better by estimating the gradients based on the other measurements.

Hence, the proposed interval field method allows to incorporate this gradient information. The method is based on Inverse Distance Weighing (IDW) with an additional set of basis functions: one set of basis functions interpolates the value, and the second set of basis functions controls the gradient at the control points. The additional basis functions can be determined in two distinct ways: first, the gradients are available or can directly be measured at the control point, and second, a weighted average is taken with respect to all control points within the domain. In general, the proposed interval field provides a more versatile definition of an interval field compared to the standard implementation of inverse distance weighting. The application of the interval field is shown in a number of one-dimensional cases where a comparison with standard inverse distance weighting is made. In addition, a case study with a set of measurement data is used to illustrate the method and how different realisations are obtained.

1 INTRODUCTION

In common engineering practice the main goal is to provide or validate component designs that should perform under a wide range of circumstances, e.g., extreme weather, impact loads, and sometimes even in space or at other planets. To ensure the performance of these components, engineers often use numerical methods to approximate the set of differential equations governing the physical behavior of the component under investigation. However, this can be a daunting task as the parameters governing these equations are often only know vaguely, as they are inherent variable, or only limited knowledge about these quantities is available, as direct

measurement is not possible, or a combination of both [1]. Hence, during the last decades a number of techniques are introduced that aim to quantify these non-deterministic quantities. In general, these techniques are categorized as probabilistic [2] and possibilistic approaches such as: intervals [3], fuzzy sets [4], and imprecise probabilities [5]. Where probabilistic methods describe non-determinism as the likelihood that parameters assume a value via a joint probability density function, possibilistic methods as, i.e. interval methods, consider non-deterministic quantities to be bounded.

In a number of cases these quantities, e.g., wind loads, Young's modulus, dielectric constants, experience a spatial or temporal dependency, which is difficult to consider within the classic interval method as described by R.E. Moore [6]. Therefore, the framework of interval fields was introduced [7], which is capable of providing the spatial or temporal dependency structure by a set of basis functions. Hence this method can be seen as a possibilistic counterpart to random fields [8]. In the last decade a number of researchers have introduced different basis functions that model the dependence structure, which can be based on inverse distance weighting [9, 10], affine arithmetic [11, 12, 13], radial basis functions [14], a spatial averaging method [15], or set-theoretical approaches [16, 17]. The basis functions that are introduced in this paper are an extension to the existing technique of inverse distance weighting, which was introduced by Sheppard [18].

In this work the focus lies on interval fields defined trough Inverse Distance Weighting (IDW), which is a very convenient way of constructing an interval field. The idea behind IDW is that the non-deterministic quantity is known or measured at independent locations within the physical domain. It is then assumed that the weight of this information decreases proportional to the inverse of the distance moving further from this measurement point, which is referred to as a control point. Although this technique is successfully applied in a number of cases it has a number of shortcomings [10], and one of such shortcomings is that the maximum value of the interval field can never exceed the maximal value placed at a control point. This property is attributed to the definition of the basis functions, which will always have a zero gradient at each of the control points. Hence, this paper proposes an interval field based on two independent sets of basis functions at each control point, where one will interpolate the value of the control points and the second set of basis basis functions will control the gradients at the control point. In general this information about the gradients may not always be available. Therefore, two methods are proposed to determine the gradients at the control points: a first method that uses direct measurement, and second a technique to estimate the gradients based on the observed trend of the data. This paper is structured as follows: in Section 2 the interval field is introduced, and in Section 3 the application of this interval field is compared with the standard technique. Finally, Section 4 illustrates a real case study and conclusions are made in section 5.

2 INTERVAL FIELD ANALYSIS

In this section a brief description of the interval field analysis is provided, for a more detailed description the reader is referred to [9]. The following definitions will be used in this paper: interval parameters are indicated using apex I: x^I; a vector is indicated as lower-case boldface character $\mathbf{x}$; matrices are expressed as upper-case boldface characters $\mathbf{X}$, and interval parameters are either represented using the bounds of the interval $x^I = [\underline{x}; \overline{x}]$ where $\underline{x}$ stands for the lower

bound and $\overline{x}$ stands for the upper bound, or by their centre point $\hat{x} = \frac{\underline{x}+\overline{x}}{2}$ and the radius $\Delta x = \frac{\overline{x}-\underline{x}}{2}$. An interval is *closed* when both the upper and lower bounds are a member of the interval. The domain of real-valued intervals is denoted as $\mathbb{IR}$.

2.1 Explicit interval fields

The definition of the proposed explicit interval field is given in Equation (1) where, opposed to the literature in [7], a second set of basis functions ϕ_i is added. The new interval field consists of the superposition of two times $n_b \in \mathbb{N}$ independent basis functions $\psi_i + \phi_i$. Here, the range of the interval is interpolated by $\psi_i : \Omega \mapsto \mathbb{R}$, and similar the gradients are determined by $\phi_i : \Omega \mapsto \mathbb{R}$. Both of these basis functions are defined over the geometrical domain $\Omega \subset \mathbb{R}^t$, where t is defined as the physical dimension of the problem. These basis functions describe the spatial nature of the non-deterministic parameter, distributed along the coordinate $\mathbf{r} \in \Omega$. An interval field is created by scaling both these basis functions $\psi_i,\ \phi_i$ with independent interval scalars $\alpha_i^I,\ \beta_i^I \in \mathbb{IR}$. This interval field is formally defined as:

$$\mathbf{x}^I(\mathbf{r}) = \hat{x} + \sum_{i=1}^{n_b} [\psi_i(\mathbf{r})\alpha_i^I + \phi_i(\mathbf{r})\beta_i^I], \tag{1}$$

with $\hat{x} \in \mathbb{R}$ the midpoint of the interval field. Note that the existing IDW framework for interval fields is a special case where $\beta_i^I = 0$. When Ω is discretised into k finite elements, these base functions ψ_i and ϕ_i interpolate the independent interval scalars α_i^I and β_i^I to dependent intervals for each element in the domain Ω. Hence, the size of the bounded uncertain input space is $2n_b$, which can be reduced when only the range or the gradient at a control point is considered, i.e., $\Delta\mathbf{x}_i = 0$ while the gradient leis between [0 1]. Nevertheless, in general this means that the input space dimension can be reduced if $2n_b < k$, which is double the amount compared to the standard method of Inverse Distance weighting (IDW).

2.2 Interval finite element analysis

A numerical model $\mathcal{M}(\mathbf{x})$ parameterised by a parameter vector $\mathbf{x}(\mathbf{r}) \in \mathcal{X} \subset \mathbb{R}^e$ is considered, with $\mathcal{X}$ the set of physically admissible parameters and $e \in \mathbb{N}$. This vector $\mathbf{x}(\mathbf{r})$ contains for instance constitutive material parameters, inertial moments or clamping stiffness that are a function of the spatial coordinate $\mathbf{r}$ over the model domain. Solving the numerical model $\mathcal{M}(\mathbf{x})$ corresponds to transforming the parameter vector $\mathbf{x}(\mathbf{r})$ through a set of function operators $m_i : \mathbb{R}^k \mapsto \mathbb{R}$ to a vector of responses $\mathbf{y}(\mathbf{r}) \in \mathcal{Y} \subset \mathbb{R}^d$, with $\mathcal{Y}$ the set of admissible model responses and $d \in \mathbb{N}$, denoted as:

$$\mathcal{M}(\mathbf{x}) : \mathbf{y}_i(\mathbf{r}) = m_i(\mathbf{x}(\mathbf{r})) \quad i = 1, \ldots, d \tag{2}$$

The dependence of $\mathbf{y}$ on $\mathbf{r}$ is only applicable for responses at the nodal or element level, which is not the case for, e.g. dynamical eigenfrequencies.

The main goal of the interval field finite element method is to find the uncertain solution set of system responses $\tilde{\mathbf{y}}$, which describes a multidimensional manifold in $\mathbb{R}^d$. Computing the exact solution is very hard as in general this manifold is non-convex. Thus, the exact solution

set $\tilde{\mathbf{y}}$ is usually approximated by an uncertain realisations set $\tilde{\mathbf{y}}_s$ defined as:

$$\tilde{\mathbf{y}}_s = \{\mathbf{y}_{sj} | \mathbf{y}_{sj} = m_i(\mathbf{x}_j(\mathbf{r})); \mathbf{x}_j(\mathbf{r}) \in \mathbf{x}^I(\mathbf{r}); j = 1, \ldots, q\}. \tag{3}$$

The set $\tilde{\mathbf{y}}_s$ is typically constructed by q deterministic solutions $\mathbf{y}_{sj}$ of the numerical model $\mathcal{M}(\mathbf{x})$, where $\mathbf{y}_{sj}$ a vector containing the d deterministic responses of the j^{th} solution. For each of these q solutions, the interval field realisations $\mathbf{x}_j^I(\mathbf{r})$ are generated by sampling the interval field. Such samples can for instance be generated by an optimisation algorithm that actively looks for the bounds in $\tilde{\mathbf{y}}$. Furthermore, the exact solution can be obtained for monotonic models when sampling the vertices of the hypercubic input space, requiring exactly 2^{n_j} evaluations [19], referred to as the vertex method. Note, that for the interval field introduced in this paper $n_j = 2n_b$, as both interval scalars are independent. However, more advanced strategies to approximate the exact solution set $\tilde{\mathbf{y}}$ are available, which can be found in [9].

2.3 Definition of the basis functions

The definition of an interval field, as presented in Equation (1) takes two basis functions, the first interpolates the range of the interval field from the control points ψ_i, and the second basis function ϕ_i controls the gradients. Through the definition of these basis functions the spatial dependence of the non-deterministic quantity of interest is modeled throughout the domain Ω. An important property of these basis functions is that they should be self-complementary, i.e. $\sum_{i=1}^{n_b} \psi_i(\mathbf{r}_j) = 1 \; \forall \; \mathbf{r}_j \in \Omega$. Furthermore, they should behave as unit vectors at the control points to ensure that independent intervals are retained (see [20] for a more thorough discussion). An intuitive definition of basis functions that comply with these requirements is provided by means of Inverse Distance Weighting (IDW) interpolation, as applied in [21], which is also used to interpolate the range at the control points to the domain Ω in this paper.

2.3.1 Basis functions for the range

The first set of basis functions is the standard IDW approach where basis functions are defined for each control point $\mathbf{r}_i$. This is accomplished by a normalisation of weight functions $w_i(\mathbf{r}) \in \Omega$, denoted as:

$$\psi_i(\mathbf{r}) = \frac{w_i(\mathbf{r})}{\sum_{j=1}^{n_b} w_j(\mathbf{r})}, \tag{4}$$

with $i = 1, \ldots, n_b$. The weight functions w_i are inversely proportional with the Euclidean distance measure $d(\cdot)$ measured between the control point $\mathbf{r}_i$ and other coordinates $\mathbf{r}$ in the domain:

$$w_i(\mathbf{r}) = \frac{1}{[d(\mathbf{r}_i, \mathbf{r})]^p}. \tag{5}$$

Herein, the power $p \in \mathbb{R}^+$ allows the analyst to influence the rate of decay of the weight function. Note that for a power $p < 1$ no derivative of the basis function exists at the control points, while in the case that $p > 2$ the basis functions flatten and higher gradients at the transitions are obtained. Empirical evidence suggests that in general $p = 2$ is a good starting point [21], if no further information about the spatial nature is available. The distance measure $d(\cdot)$ is measured in Euclidean space, defined as:

$$d(\mathbf{r}_i, \mathbf{r}) = \|\mathbf{r}_i - \mathbf{r}\|_2 , \tag{6}$$

with $\|\cdot\|_2$ denoting the L_2 norm.

2.3.2 Basis functions for the gradient

The second set of basis functions is constructed in a similar manner as the IDW basis functions and identical weight functions are used, as they assign a higher weight to points in $\mathbf{r}$ closer to a control point $\mathbf{r}_i$. These basis functions are defined as:

$$\phi_i(\mathbf{r}) = \frac{w_i(\mathbf{r})\delta_i(\mathbf{r})}{\sum_{j=1}^{n_b} w_j(\mathbf{r})}, \tag{7}$$

with $\delta_i : \mathbb{R} \mapsto \mathbb{R}$ a factor to set the gradients at the control points $\mathbf{r}_i$, which is defined as:

$$\delta_i = A_i(\mathbf{r} - \mathbf{r}_i)\left[\frac{R_i}{R_i + d(\mathbf{r}_i, \mathbf{r})}\right], \tag{8}$$

here $A_i \in \mathbb{R}_+$ represents the desired gradient at the control point and the constant $R_i \in \mathbb{R}_+$ is a scaling factor, defined as:

$$R_i = \frac{v(\max(\hat{\mathbf{x}}_i) - \min(\hat{\mathbf{x}}_i))}{A_i}, \tag{9}$$

where the parameter $v \in \mathbb{R}_+$ is a parameter that bounds the effect of the gradient terms on the final interpolated value, and should be defined by the user. The value $|\delta_i(\mathbf{r})|$ that is added by these basis functions ϕ_i causes the derivatives to be $\frac{\partial \delta_i}{\partial r} = A_i$. This is only valid at the control points as the value of $\phi_i(\mathbf{r})$ for consecutive points moving away from $\mathbf{r}_i$ as the factor $R_i/\left[R_i + d(\mathbf{r}_i, \mathbf{r})\right]$ will go from 1 to behaving like $d(\mathbf{r}_i, \mathbf{r})^{-1}$ for large $d(\cdot)$. In addition, note that $\delta_i(\mathbf{r}_i) = 0$ thus keeping the independence of the basis functions at the control points, which can therefore be scaled by independent interval scalars while retaining the self-complementary basis and the independency of the intervals scalars at the control points. However, note that these basis functions are not self complementary beyond the control points.

The only remaining parameter is the constant A_i which will be the gradient at the control point. Depending on the available data two distinct ways of calculating A_i are presented. The first method is to directly calculate the constant based of points close to $\mathbf{r}_i$, defined as:

$$A_i = \frac{(\hat{\mathbf{x}}_j - \hat{\mathbf{x}}_i)(\mathbf{r}_i - \mathbf{r}_j)}{d(\mathbf{r}_i, \mathbf{r}_j)^2}, \tag{10}$$

here the index j is given to a neighbouring point $\mathbf{r}_{i\pm j}$ used to calculate the constant A_i. Depending on the side and the distance the result of equation (10) can differ, in this case the maximal value is taken. In this case the assumption is made that there is more information available around the control points, which may not be the case in general.

Therefore, a second approach is to determine the constants A_i as a weighted average of the control points $\mathbf{r}_j \in \mathbf{r}_i$, defined as:

$$A_i = \frac{\sum_j^{n_b} w_i \frac{(\hat{\mathbf{x}}_j - \hat{\mathbf{x}}_i)(\mathbf{r}_i - \mathbf{r}_j)}{d(\mathbf{r}_i, \mathbf{r}_j)^2}}{\sum_j^{n_b} w_j}, \tag{11}$$

where the weights w_j are defined as in equation (5), which assigns less weight to control points far from $\mathbf{r}_i$. Furthermore, in this work A_i is determined based on the midpoint $\hat{x}$ of the intervals, which will give an average gradient that is acceptable for a large number of cases. However, it is easy to define a case with increasing non-determinism with a zero midpoint, thus depending on the case better results can be obtained by changing this to the interval radius Δx, or the extremes of the interval $\overline{x}_i$, $\underline{x}_i$. Using these basis functions will ensure that the desired derivatives A_i are obtained at each control point $\mathbf{r}_i$.

One of the important things to note here is that the basis functions ϕ_i of the gradients add a value $|\delta_i(\mathbf{r})|$ to the standard IWD basis functions ψ_i. This value of $|\delta_i(\mathbf{r})|$ is zero at the control points, and can be changed between the control points this by setting the parameter v, which changes the value of $|\delta_i|$ as:

$$|\delta_i(\mathbf{r})| \leq v[\max(\Delta\mathbf{x}_{i\pm j}) - \min(\Delta\mathbf{x}_{i\pm j})], \tag{12}$$

with the index $j \in \mathbf{r}_i \pm r$. The implication of using the basis functions ϕ_i that the maximum value of the interval field is no longer restricted to the location of a control point and can be anywhere within the domain Ω.

3 ILLUSTRATION OF INTERVAL FIELDS WITH LOCAL GRADIENT CONTROL

The following cases compare and illustrate the use of the novel interval technique. First a comparison is made with the existing IDW technique, second the two different strategies for calculating are explored, and the third case is about extracting samples and the possibilities towards dependence structures between α^I and β^I.

3.1 Comparison between IDW with and without gradient control

To demonstrate the additional value of incorporating gradient information in the basis functions a case is considered where only limited information about a set of measurements is available. This set $\mathcal{A}$ represents the true underlying spatial non-determinism for a parameter, e.g., used in the finite element method. The measurements are made at the points [0.01, 0.15, 0.8], which are therefore also used as the control points $\mathbf{r}_i$ of the interval field. In order to calculate the first basis functions that will interpolate the range at the control points ψ_i, the parameter p is set to $p = 2$. figure 1a illustrates the basis functions that are obtained, which are 1 at the location of the control point.

The second set of basis functions ϕ_i provides the desired spatial gradients at the control points, which are calculated exactly from the midpoint $\hat{\mathbf{x}}_i$ of the set $\mathcal{A}$. The motivation is that these points represent a small group of measurements or this can be based on engineering judgement. Hence, the basis functions are calculated following equation (7) where the spatial gradients are taken from equation (10). In this case the parameter v is set at 10, which is an arbitrary choice. The obtained basis functions are shown in Figure 1b, where these are zero at the control points. Note that these basis functions are not self complementary $\sum_1^{nb} \phi_i \neq 1 \; \forall \; i$ outside the control points. In Figure 1c the sum of these basis functions is given with the interval scalars set at one $\alpha_i^I, \beta_i^I = 1$.

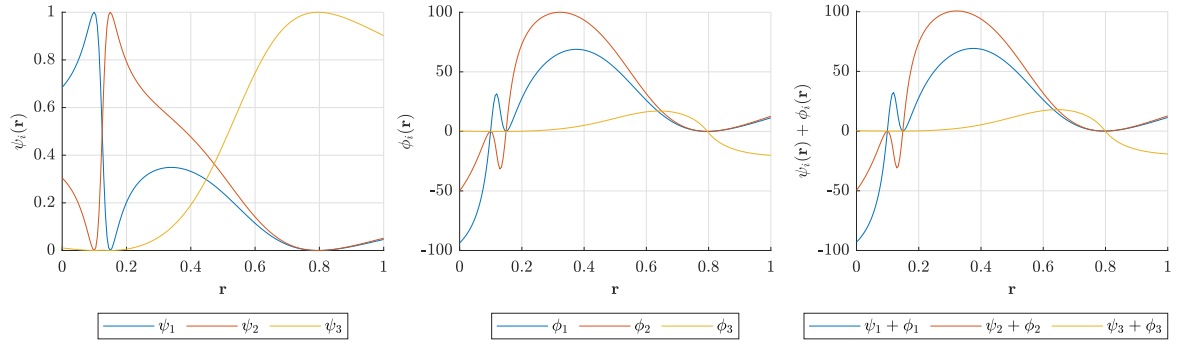

(a) Basis functions for the interval field value

(b) Basis functions for the derivative

(c) Sum of the basis functions without scalars

Figure 1: Basis functions obtained by exact calculation of the derivatives, as indicated by equation (10)

Figure 2a illustrates the outer realisations, in red and blue lines, and the vertex realisations, in dashed lines, of the interval scalar α^I. Hence, we are only considering the combinations of different values without different gradients, as indeed β^I can also vary between $[-1\ 1]$ causing the gradients to lie within the interval $[-A_i\ A_i]$. Therefore, the illustrations in this case and the following case are limited to $\beta^I = 1$, which will set the gradients at the control points equal to the calculated values of A_i.

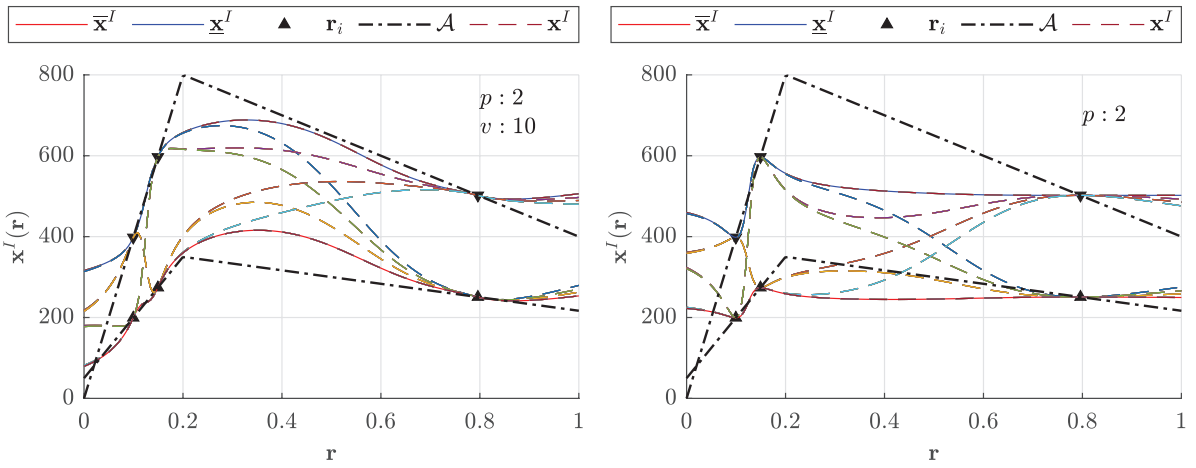

(a) Interval field using the derivatives

(b) Interval field using IDW

Figure 2: Vertex realisations of an interval field based on IDW (b) and one using the information about the derivatives (a); the dash-dotted line indicates the unknown underlying uncertainty

In Figure 2b a similar plot is made with the standard IDW basis functions, which are identical

to ψ_i. A comparison between Figure 2a and 2b shows that the proposed method is capable of capturing the gradients and thus provides a better estimation of the set $\mathcal{A}$. In addition, one can see that the maximum value of the interval field based on IDW is located at the control point where in Figure 2a this is located between $\mathbf{r}_2$ and $\mathbf{r}_3$, which is an intuitive location based on the gradient information at the control points.

3.2 Determination of the gradient from other control points

In the previous case the gradients are directly calculated at the control points, which requires additional information at the control points, which may not be available. Therefore, a different approach is considered where the constants A_i are calculated based on a weighted average of the midpoints, as described in equations (11). The basis functions that are obtained in this way are given in Figure 3 where the first illustration 3a is identical to this in 1a. However, looking at the basis functions of the gradients ϕ_i it show a gradient close to zero for the third control point $\mathbf{r}_3$, which is attributed to the distance and the small relative change of midpoint at these locations.

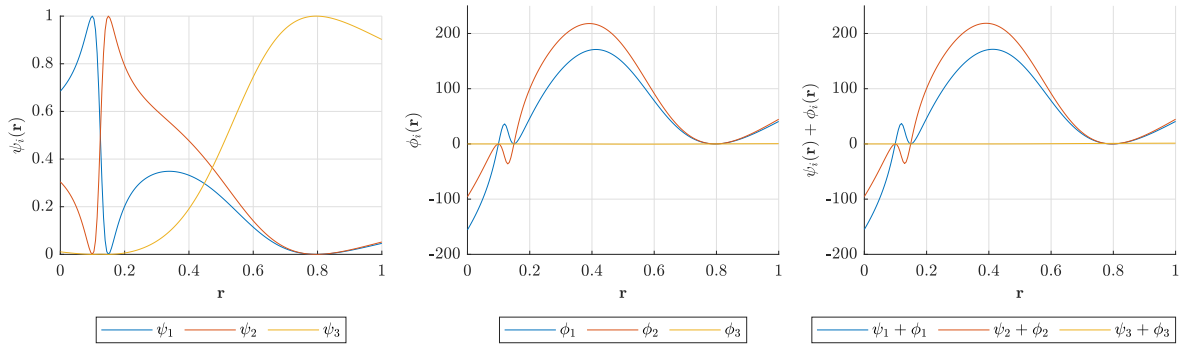

(a) Basis functions for the interval field value

(b) Basis functions for the derivative

(c) Sum of the basis functions without scalars

Figure 3: Basis functions based on the derivatives calculated from the information at the other control points, as described by (11)

In Figure 4 the realisations of this interval field are given, which have a higher maximum value compared to the previous case without changing the value of v. This effect is also seen in the basis function in Figure 3b, which have a maximal value almost double as high as the previous basis functions. This is caused by the larger difference in the values that are used to calculate the constants, which is described by (12) and can be changed by selecting a different value v.

3.3 Interval field realisations

As described in the first case, each of the realisations until here are given with vertex samples from α^I, while $\beta^I = 1$ is kept constant. However, this interval field consists of a two-dimensional

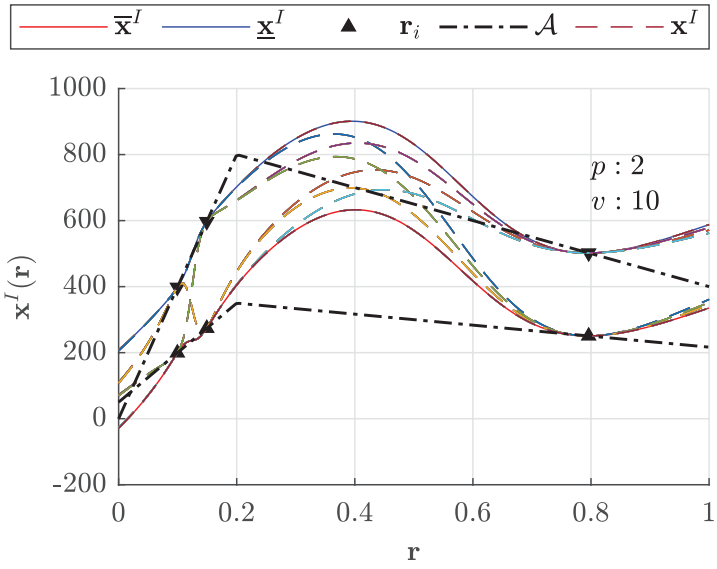

Figure 4: Realisations case 1

uncertain input space at each control point. Thus, a full vertex analysis consists out of 2^{2n_b} samples. In addition, it is up to the analysis to determine the range of the gradients as these can vary between $[-A_i \ A_i]$ illustrated in Figure 5a where the sign of the gradient is unknown at the control points and there are a large number of possible realisations. It is also possible to limit the values in β^I from $[0 \ A_i]$ as shown in Figure 5b where the gradients are equal to A_i or smaller.

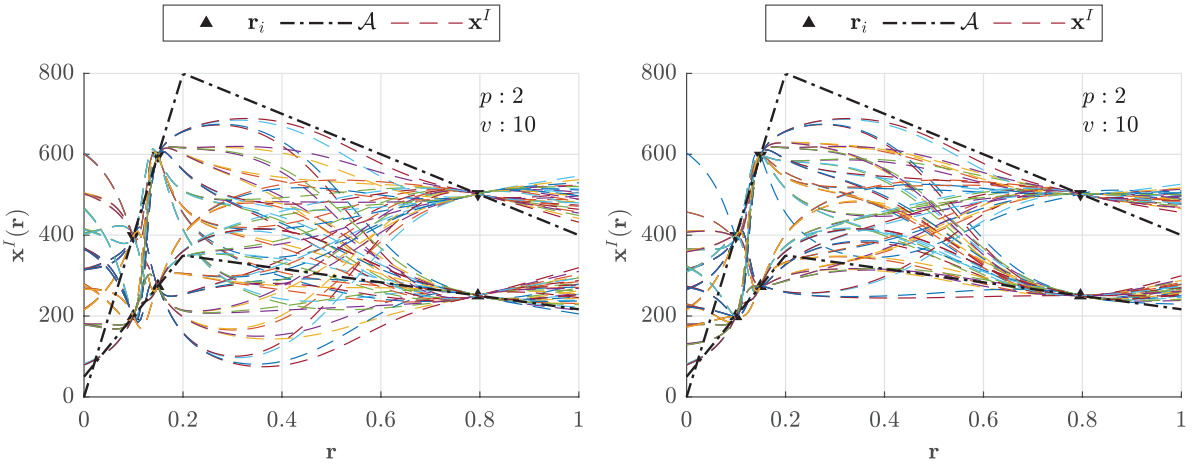

(a) Vertex realisation for both $\alpha^I, \beta^I \in [-1 \ 1]$ (b) Vertex realisation for $\alpha^I \in [-1 \ 1]$ and $\beta^I \in [0 \ 1]$

Figure 5: two realisations of an interval field representing the envelope $\mathcal{A}$

It is clear from Figure 5a that the possible values of the gradients should be limited in this case as a large number of realisations leis outside the data $\mathcal{A}$. Although, limiting β^I to lie within an interval $[A_i\ 0]$ it should be noted that more complex dependency structures could be defined, as described in [9]. Nevertheless, one should always define an interval for β^I as keeping β^I at a fixed value will fully couple the value at a control point with the gradient, which is not the case in general.

4 CASE STUDY

In this final case study the method is applied to capture the non-determinism of a set of stress-strain curves. The objective is to represent the set of measurements with an interval field, and each sample of this interval field should represent a feasible stress-strain curve. To obtain the stress-strain curves provided in Figure 6a three samples have been printed and tested under uni-axial tension, in accordance with ASTM D638.

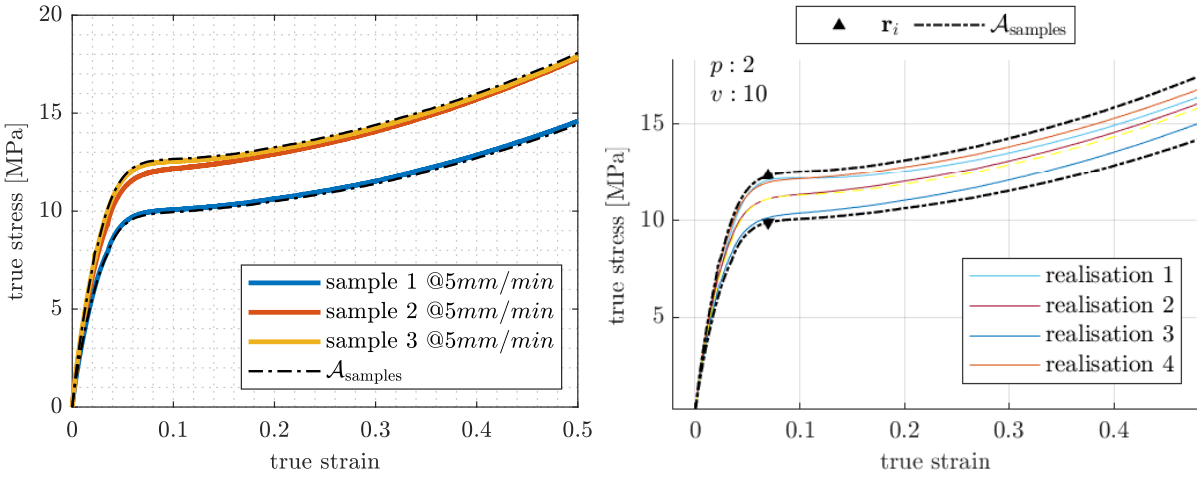

Figure 6: Measured stress-strain curves (a) and the interval field representation (b); the dashed line represents the envelope $\mathcal{A}_{\text{samples}}$

To illustrate the additional value of the method only two control points are placed, one at the origin and one at $r = 0.07$. The constant A_i are in this case calculated at each point directly, following Equation (10), based on the interval radius Δx of $\mathcal{A}_{\text{samples}}$. The resulting interval field shown in Figure 6b in only sampled at $\beta_1^I = 0, -0.5, -0.5, -1$ and $\alpha_2^I = 0.8, 0, -0.8, 0.7$ labeled realisations $1, 2, 3$ and 4, respectfully. Thus, the non-deterministic measurement set is represented only using the gradient at the first control point and the value at the second control point, which could be regarded as sampling the initial stiffness of the material and the yield strength.

This case is used as an example where the parameters and control points are set by hand. In a more comprehensive study to find the optimal interval field to represent a set of measurements optimisation approaches can be used, as in [22]. Furthermore, detailed investigations into the

set of admissible realisations need to be made.

5 CONCLUSIONS

In this paper an extension to the existing framework of interval fields is presented. This extension allows for the incorporation of information about gradients at the control points. It is shown that this method is better capable in representing a spatially distributed non-deterministic quantity compared with the existing technique. Even without explicit information about the gradients at the control points better agreement is obtained by making an estimation about these gradients. The control the effects a parameter v is introduced that allows the user to adjust the realisations of the interval field by tuning the influence of the gradients on the final result. In addition, a case study is conducted with a set of real measurements, which could be represented using only the gradient information in one control point and the range at the other control point. Further research will focus on the application of admissible set decomposition, which allows for dependency structures within the interval framework.

ACKNOWLEDGEMENTS

The authors gratefully acknowledge the support of the Research Foundation Flanders (FWO) under grant 1SA3919N (C. van Mierlo).

REFERENCES

[1] Scott Ferson and Lev R. Ginzburg. Different methods are needed to propagate ignorance and variability. *Reliability Engineering and System Safety*, 54(2-3):133–144, 1996.

[2] George Stefanou. The stochastic finite element method: Past, present and future. *Computer Methods in Applied Mechanics and Engineering*, 198(9-12):1031–1051, 2009.

[3] Matthias Faes, Matteo Broggi, Edoardo Patelli, Yves Govers, John Mottershead, Michael Beer, and David Moens. A multivariate interval approach for inverse uncertainty quantification with limited experimental data. *Mechanical Systems and Signal Processing*, 118:534 – 548, 2019.

[4] Michael Hanss. *Applied fuzzy arithmetic*. Springer, 2005.

[5] Michael Beer, Scott Ferson, and Vladik Kreinovich. Imprecise probabilities in engineering analyses. *Mechanical systems and signal processing*, 37(1-2):4–29, 2013.

[6] Ramon E Moore. *Interval analysis*, volume 4. Prentice-Hall Englewood Cliffs, 1966.

[7] D. Moens, M. De Munck, W. Desmet, and D. Vandepitte. Numerical dynamic analysis of uncertain mechanical structures based on interval fields. In Alexander K. Belyaev and Robin S. Langley, editors, *IUTAM Symposium on the Vibration Analysis of Structures with Uncertainties*, pages 71–83, Dordrecht, 2011. Springer Netherlands.

[8] Erik Vanmarcke. *Random fields: analysis and synthesis*. World Scientific, 2010.

[9] Matthias Faes and David Moens. Recent trends in the modeling and quantification of non-probabilistic uncertainty. *Archives of Computational Methods in Engineering*, 27(3):633–671, 2020.

[10] Conradus van Mierlo, Matthias G.R. Faes, and David Moens. Inhomogeneous interval fields based on scaled inverse distance weighting interpolation. *Computer Methods in Applied Mechanics and Engineering*, 373:113542, 2021.

[11] Alba Sofi. Structural response variability under spatially dependent uncertainty: Stochastic versus interval model. *Probabilistic Engineering Mechanics*, 42:78 – 86, 2015.

[12] Alba Sofi, Giuseppe Muscolino, and Isaac Elishakoff. Static response bounds of Timoshenko beams with spatially varying interval uncertainties. *Acta mechanica*, 226:3737–3748, 2015.

[13] Alba Sofi, Eugenia Romeo, Olga Barrera, and Alan Cocks. An interval finite element method for the analysis of structures with spatially varying uncertainties. *Advances in Engineering Software*, 128:1–19, 2018.

[14] Maurice Imholz, Dirk Vandepitte, and David Moens. Derivation of an input interval field decomposition based on expert knowledge using locally defined basis functions. In *1st ECCOMAS Thematic conference on international conference on uncertainty quantification in computational sciences and engineering*, pages 1–19, 2015.

[15] Di Wu and Wei Gao. Hybrid uncertain static analysis with random and interval fields. *Computer Methods in Applied Mechanics and Engineering*, 315:222–246, 2017.

[16] Chao Jiang, Bingyu Ni, Ningyu Liu, Xu Han, and Jie Liu. Interval process model and non-random vibration analysis. *Journal of Sound and Vibration*, 373:104–131, 2016.

[17] Bingyu Ni and Chao Jiang. Interval field model and interval finite element analysis. *Computer Methods in Applied Mechanics and Engineering*, 360:112713, 2020.

[18] Donald Shepard. A two-dimensional interpolation function for irregularly-spaced data. In *Proceedings of the 1968 23rd ACM National Conference*, ACM '68, page 517–524, New York, NY, USA, 1968. Association for Computing Machinery.

[19] Michael Hanss. The transformation method for the simulation and analysis of systems with uncertain parameters. *Fuzzy Sets and Systems*, 130(3):277 – 289, 2002.

[20] Matthias Faes and David Moens. On auto- and cross-interdependence in interval field finite element analysis. *International Journal for Numerical Methods in Engineering*, (February):nme.6297, jan 2020.

[21] Matthias Faes and David Moens. Identification and quantification of spatial interval uncertainty in numerical models. *Computers & Structures*, 192:16–33, 2017.

[22] Conradus van Mierlo, Matthias GR Faes, and David Moens. Inhomogeneous interval fields based on scaled inverse distance weighting interpolation. *Computer Methods in Applied Mechanics and Engineering*, 373:113542, 2021.